

THE EFFECT OF LOW DOSE RATE IRRADIATION ON THE TENSILE PROPERTIES AND MICROSTRUCTURE OF AUSTENITIC STAINLESS STEELS

T.R. Allen, H. Tsai, and J. I. Cole, Argonne National Laboratory, U.S.A.

T. Yoshitake, N. Akasaka, T. Donomae, and S. Mizuta, Japan Nuclear Cycle Development Institute, Japan

J. Ohta, K. Dohi, and H. Kusanagi, Central Research Institute of Electric Power Industry, Japan

Abstract

To assess the effects of long-term, low-dose-rate neutron exposure on mechanical strength and ductility, tensile properties were measured on 12% and 20% cold-worked Type 316 stainless steel. Samples were prepared from reactor core components retrieved from the EBR-II reactor following final shutdown. Sample locations were chosen to cover a dose range of 1-56 dpa at temperatures from 371-440°C and dose rates from $0.5-5.8 \times 10^{-7}$ dpa/s. These dose rates are approximately an order of magnitude lower than those of typical EBR-II test sample locations. The tensile tests for the 12% CW material were performed at 380°C and 430°C while those for the 20% CW samples were performed at 370°C. In each case, the tensile test temperature approximately matched the irradiation temperature. To help understand the tensile properties, microstructural samples with similar irradiation history were also examined. The strength and loss of work hardening increase the fastest as a function of irradiation dose for the 12% CW material irradiated at lower temperature. The decrease in ductility with increasing dose occurs more rapidly for the 12% CW material irradiated at lower temperature and the 20% cold-worked material. Post-tensile test fractography indicates that at higher dose, the 20% CW samples begin a shift in fracture mode from purely ductile to mainly small facets and slip bands, suggesting a transition toward channel fracture. The fracture for all of the 12% cold-worked samples was ductile. For both the 12% and 20% CW materials, the yield strength increases correlate with changes in void and loop density and size.

Background

The objective of this research was to evaluate the effects of long-term, low dose-rate neutron exposure on the tensile and fracture properties and associated microstructural changes in 12% and 20% cold worked Type 316 stainless steel. The majority of information available on the effect of radiation on Type 316 stainless steel comes from experiments performed in the driver (fueled) regions of the EBR-II reactor, where dose rates are on the order of 1×10^{-6} dpa/s (see figure 1). The material analyzed in this study came from 1-mm thick subassemblies (hex cans) irradiated in rows 8 and 9 of the reflector region of EBR-II. The displacement rates in rows 8 and 9 are about an order of magnitude lower than in the fueled region of the core. Analysis of reflector components removed from the reactor following final shutdown provides a valuable source of information on behavior of reactor structural materials irradiated at dose rates on the order of 10^{-7} - 10^{-8} dpa/s. This analysis will provide data on radiation-induced degradation in low dose rate, possibly non-replaceable, core components in light water and fast reactors.

Experiment

The materials studied were 12% and 20% cold-worked AISI 316 stainless steel. In this study, the results of tensile tests and associated fractography and microstructural characterization are reported. Table 1 lists the irradiation conditions for the samples analyzed and reported in this work. The 12% cold-worked 316 was irradiated and tested at $\sim 380^\circ\text{C}$ and $\sim 430^\circ\text{C}$. The 20% cold-worked 316 was irradiated and tested at $\sim 370^\circ\text{C}$. A full description of sample preparation, test, and analysis steps can be found in references [1-4].

To form a direct comparison with a prior study [5] on irradiated 20% cold-worked Type 316 stainless steel irradiated at higher dose rate, the strain rate for 20% CW tensile tests was $4 \times 10^{-5}/\text{s}$, the same as the prior study. The strain rate for the 12% CW samples was $1 \times 10^{-3}/\text{s}$. At these temperatures, the difference in strain rates between the 12% and 20% CW tests is not expected to significantly change the measured mechanical properties [6].

Results and Discussion

The yield strength as a function of irradiation dose is shown in figure 2. The yield strength increases most rapidly for the 12% cold-worked 316 irradiated and tested at lower ($\sim 380^\circ\text{C}$) temperature. The majority of the increase in yield strength appears to occur over about the first 10 dpa of irradiation. The increase in yield strength as a function of dose is similar for the 12% cold-worked 316 irradiated and tested at higher temperature ($\sim 430^\circ\text{C}$) and for the 20% cold-worked 316. For these two conditions, the increase in yield strength occurs more slowly as a function of irradiation dose. For the 12% cold-worked 316 irradiated at ~ 430 , there is a fairly large scatter in the measured yield strength at any specific dose. The ultimate tensile strength (not shown), follows similar trends as the yield strength for all three conditions.

The ductility, as measured by the total elongation to failure, is presented in figure 3. The total elongation for the 12% cold-worked 316 irradiated and tested at lower ($\sim 380^\circ\text{C}$) temperature decreases rapidly over the first 10 dpa. A similar effect occurs for the 20% cold-worked 316. At the highest dpa achieved for the 20% cold-worked 316 (47 dpa), the total elongation at failure is around 2%, which is quite low. The decrease in total elongation is the slowest for the 12% cold-worked 316 irradiated and tested at higher temperature ($\sim 430^\circ\text{C}$). Trends in the ultimate tensile strength (not shown) were similar to the total elongation.

A measure of the ability to work harden is the quantity $\left(1 - \frac{\sigma_y}{\sigma_u}\right)$, where σ_y is the yield strength

and σ_u is the ultimate tensile strength. As the material hardens, the yield strength approaches the ultimate tensile strength. This quantity is plotted as a function of dose in figure 4. Figure 4 includes data for the 12% cold-worked 316 irradiated and tested at lower ($\sim 380^\circ\text{C}$) temperature, the 12% cold-worked 316 irradiated and tested at higher ($\sim 430^\circ\text{C}$) temperature, and the 20% cold-worked 316. In addition, data from Fish et al., [5] on the hardening of 20% cold-worked 316 irradiated at high dose rate in row 2 of EBR-II is included in figure 4. The 12% cold-worked 316 irradiated and tested at lower ($\sim 380^\circ\text{C}$) temperature and the 20% cold-worked 316 irradiated

at high dose rate (from Fish et al.) harden the fastest. At high dose, it appears all of the alloys approach a similar value of around 0.05 (where the yield strength is ~95% of the ultimate tensile strength).

The low total elongation of the 20% cold-worked samples tested in this study correlates with a change in fracture mode. Posttest fractography was performed on two representative samples of the 20% cold-worked material at doses of 30 and 47 dpa using a scanning electron microscope. Necking of the gauge section in the 30 dpa specimen is evident, but for the higher-dose specimen, necking is almost imperceptible. This is consistent with the measured elongation data, which showed further reduction of ductility during irradiation from 30 to 47 dpa. Because necking constitutes a sizable fraction of the gauge deformation after the maximum load (uniform elongation) is attained before fracture, it reflects to a large extent the difference between the uniform and total elongation.

Fracture in the 20% cold-worked specimen irradiated to 30 dpa is mainly ductile but with local regions of mixed-mode failure. The ductile fracture, illustrated in (Figure 5), consists mainly of dimples and microvoids. Among the dimples, there are facet features that suggest flow localization and slip band decohesion. The 30 dpa sample has limited areas with mixed mode fracture (not shown) where some failure appears as a transgranular shear along active slip planes. The side surface of the 30 dpa specimen shows steps from the tensile deformation; such features are typically associated with dislocation channeling in material.

The fracture surface of the higher-exposure 47 dpa specimen displays significantly more brittle features, as shown in Figure 6. The fracture consists of mainly small facets and slip bands that suggest channel fracture. Dimples and microvoids are far less abundant than in the lower-exposure 30 dpa specimen. Noticeable steps are also found on the side surfaces of the specimens.

Post-tensile test fractography was also performed on 12% cold-worked samples. Fractography was performed on samples irradiated to doses from 19-41 dpa at temperatures of 417-435°C to elucidate the fracture mode and to determine the cross-sectional reduction-in-areas. Frontal view of the fracture tips revealed necking of the gauge section in both the thickness and width directions. Similar necking deformation was seen in the other three specimens on the SEM. The relatively high reduction-in-areas, 27% for a 30 dpa/425°C sample and 36% for samples irradiated to 19 dpa/435°C, 30 dpa/425°C, and 41 dpa/417°C, agree with the substantial elongations for 12% cold-worked 316 irradiated ~430°C. Further corroborating the observation that the material after the irradiation was still ductile, the SEM fractography confirmed that the fracture consisted of exclusively ductile dimples and microvoids in all four specimens. No channel facets or other brittle features were present in any of the surfaces examined.

The void and Frank loop size distributions were measured in both 12% and 20% cold-worked 316 samples following irradiation. The microstructures for the 12% cold-worked material were only characterized for the higher temperature (~430°C) samples. The average size along with the measured density is listed in Table 2. These irradiation-induced defects are known to cause hardening. The hardening from each defect can be estimated from dispersed hardening theory [7]. The change in yield strength due to discrete obstacles is given by:

$$\Delta\sigma_y = M\alpha\mu b\sqrt{Nd} \quad (1)$$

where M relates the shear stresses on a slip plane in a single crystal to the applied tensile stress necessary to activate slip in a polycrystal, α is the barrier strength, μ is the shear modulus of the matrix, b is the Burgers vector of a moving dislocation, N is the number density, and d the average diameter. The inverse of the quantity \sqrt{Nd} represents average obstacle spacing.

The increment in yield strength due to loops and voids is typically calculated using a root-mean-square summation:

$$(\Delta\sigma_y^{\text{voids+loops}} = \sqrt{(\Delta\sigma_y^{\text{voids}})^2 + (\Delta\sigma_y^{\text{loops}})^2}) \quad (2)$$

Figure 7 shows the calculated yield strength increment based on the measured loop and void size distributions. The values of α and μ used to calculate the yield strength increment are taken from Reference [7] and listed in Table 3. The values of M and b used to calculate the yield strength increment are taken from Reference [8] and are also listed in Table 3.

Comparing figure 2 and figure 7, the yield strength increment from the loops and voids slowly increases with dose in a manner similar to the changes in yield strength. The increment due to loops and voids are only a part of the total yield strength. In addition, network dislocations and precipitates also contribute to increases above the inherent yield strength in the solution annealed state. Examining figure 7, the yield strength increment from loops and voids is larger than the change in measured yield strength. Concurrent with the buildup of radiation-induced defects, a portion of the network dislocations present in the cold-worked material in the unirradiated state anneal out during the long-time low-dose rate irradiation [9]. This decrease in network dislocation density leads to a net decrease in yield strength that occurs at the same time as the increases due to radiation-induced defects.

CONCLUSIONS

Mechanical properties and associated microstructural changes were measured on cold-worked AISI 316 stainless steel irradiated under low dose rate conditions. Both 12% and 20% cold-worked conditions were examined. Although the yield strength for each condition approached similar values with increasing dose, the rate of increase in strength differed with cold-work and irradiation temperature. The 12% cold-worked steel irradiated and tested at lower temperature ($\sim 380^\circ\text{C}$) had the fastest rate of strength increase. Differences in elongation were also noted. The 12% cold-worked steel irradiated and tested at lower temperature ($\sim 380^\circ\text{C}$) and the 20% cold-worked 316 had the fastest rate of decrease in total elongation. The total elongation for the 20% cold-worked stainless steel reached 2% at 47 dpa, a low value. At this high dose and low elongation, the fracture was starting to transition from ductile to a more channeled fracture. Changes in Frank loop and void density were consistent with the changes in yield strength.

ACKNOWLEDGEMENTS

The authors gratefully acknowledge the efforts of M. E. Vaughn, J. P. Webb, E. L. Wood, and the staffs at the Hot Fuels Examination Facility at ANL-West. Thanks to K. A. Bunde for performing dose calculations and to R. T. Jensen for performing temperature calculations. Work supported under contract W-31-109-Eng-38 with the Department of Energy.

REFERENCES

- [1] T. Yoshitake, T. Donomae, S. Mizuta, H. Tsai, Robert V. Strain, T.R. Allen, and J.I. Cole, "Tensile Properties of 12% Cold-Worked 316 Stainless Steel Irradiated at EBR-II Reactor with Lower Dose Rate Conditions to High Fluence," *Effects of Radiation on Materials: 20th International Symposium*, ASTM STP 1405, S. T. Rosinski, M. L. Grossbeck, T. R. Allen, and A. S. Kumar, Eds., American Society for Testing and Materials, West Conshohocken, PA 2002, p. 469.
- [2] T. R. Allen, H. Tsai, J. I. Cole, J. Ohta, K. Dohi, H. Kusanagi,., "**Properties of 20% Cold-Worked 316 Stainless Steel Irradiated at Low Dose Rate**," *Effects of Radiation on Materials, ASTM STP 1447*, M. L. Grossbeck, T. R. Allen, R. G. Lott, and A. S. Kumar, Eds., ASTM International, West Conshohocken, PA, 2003
- [3] T. R. Allen, J. I. Cole, H. Tsai, S. Ukai, S. Mizuta, and T. Yoshitake, The Effect of Low Dose Rate Irradiation on the Swelling of 12% Cold-Worked 316 Stainless Steel, *Proceedings of the Ninth International Symposium on Environmental Degradation of Materials in Nuclear Power Systems-Water Reactors*, , S. Bruemmer, P. Ford, G. Was Eds., Newport Beach, CA, TMS, Warrendale, PA, (August 1999), p.1035.
- [4] J. I. Cole, T. R. Allen, H. Kusanagi, K. Dohi, and J. Ohta "Microstructure and Post-irradiation annealing Behavior of 20% Cold-worked 316 Stainless Steel," Proceedings of the MRS Fall Meeting: Microstructure Processes in Irradiated Materials-2000, Vol. 650, Materials Research Society, Warrendale, PA, p. R3.12.
- [5] Fish, R. L., Cannon, N. S., and Wire, G. L., "Tensile Property Correlations for Highly Irradiated 20 Percent Cold-Worked Type 316 Stainless Steel", *Effects of Radiation on Structural Materials, ASTM STP 683*, 1979, p. 450.
- [6] ASTM reference on strain rate.
- [7] Lucas, G. E., *Journal of Nuclear Materials*. **206** (1993) pp. 287-305.
- [8] Garner, F., Hamilton, M., Panayotou, N., and Johnson, G., *Journal of Nuclear Materials*. 103/104 (1981) p. 803.
- [9] T. R. Allen and J. I. Cole, H. Tsai, T. Yoshitake, T. Donamae, N. Akasaka, Mechanical properties and microstructural development in irradiated 316 stainless steel, 16th International Conference on Structural Materials in Reactor Technology (SmiRT-16) Washington, DC August 12-17, 2001, Paper G11/6.

Table 1. Sample conditions

Material	Sample Type	Dose (dpa)	Irrad Temp. (°C)	Tensile Test Temp. (°C)
20 % CW	TEM	1	373	NA
20 % CW	TEM	20	375	NA
20 % CW	TEM	30	379	NA
20 % CW	Tensile	1	371	370
20 % CW	Tensile	1	371	370
20 % CW	Tensile	20	375	370
20 % CW	Tensile	20	375	370
20 % CW	Tensile	30	376	370
20 % CW	Tensile	30	376	370
20 % CW	Tensile	47	385	370
20 % CW	Tensile	47	385	370
12 % CW	TEM	23	376	NA
12 % CW	TEM	23	377	NA
12 % CW	TEM	25	430	NA
12 % CW	TEM	25	429	NA
12 % CW	TEM	36	408	NA
12 % CW	TEM	36	414	NA
12 % CW	TEM	50	394	NA
12 % CW	TEM	50	397	NA
12 % CW	TEM	51	407	NA
12 % CW	Tensile	1	371	380
12 % CW	Tensile	9	374	380
12 % CW	Tensile	14	375	380
12 % CW	Tensile	0	430	430
12 % CW	Tensile	9	444	430
12 % CW	Tensile	14	436	430
12 % CW	Tensile	14	438	430
12 % CW	Tensile	19	432	430
12 % CW	Tensile	19	435	430
12 % CW	Tensile	20	432	430
12 % CW	Tensile	30	417	430
12 % CW	Tensile	30	422	430
12 % CW	Tensile	30	425	430
12 % CW	Tensile	30	425	430
12 % CW	Tensile	41	409	430
12 % CW	Tensile	41	417	430

Table 2. Cavity and Dislocation Loop Data for Duct Material

			Voids		Frank Loops	
Material	Temp (°C)	Dose (dpa)	Density, m ⁻³	Average Diameter, (nm)	Density, m ⁻³	Average Diameter, (nm)
20% CW	373	1	N/A	N/A	6.0 x 10 ²⁰	22
20% CW	375	20	1.2 x 10 ²¹	9.9	3.4 x 10 ²¹	26
20% CW	376	30	1.0 x 10 ²¹	11.1	2.1 x 10 ²¹	27
12% CW	376	23.2	3.2 x 10 ²¹	6.1	2.2 x 10 ²¹	21.5
12% CW	377	23.7	4.4 x 10 ²¹	10.0	1.0 x 10 ²¹	25.0
12% CW	394	49.5	5.4 x 10 ²¹	12.9	1.3 x 10 ²¹	26.2
12% CW	397	49.7	1.3 x 10 ²²	12.2	3.0 x 10 ²¹	21.5
12% CW	407	51.1	7.9 x 10 ²¹	14.1	1.5 x 10 ²¹	28.3
12% CW	408	35.7	4.8 x 10 ²¹	6.1	6.8 x 10 ²¹	24.7
12% CW	414	35.7	2.6 x 10 ²¹	8.8	8.2 x 10 ²¹	32.9
12% CW	430	24.5	<1 x 10 ²¹	< 10 nm	1.2 x 10 ²¹	44.7
12% CW	429	24.7	8.5 x 10 ²⁰	16.0	4.9 x 10 ²⁰	36.4

Table 3 - Constants for Yield Strength Increment Calculations

Parameter	Voids	Loops
M	3	3
α	1	0.33
μ	6.7x10 ¹⁰ Pa	6.7x10 ¹⁰ Pa
b	2.5x10 ⁻¹⁰ m	2.5x10 ⁻¹⁰ m

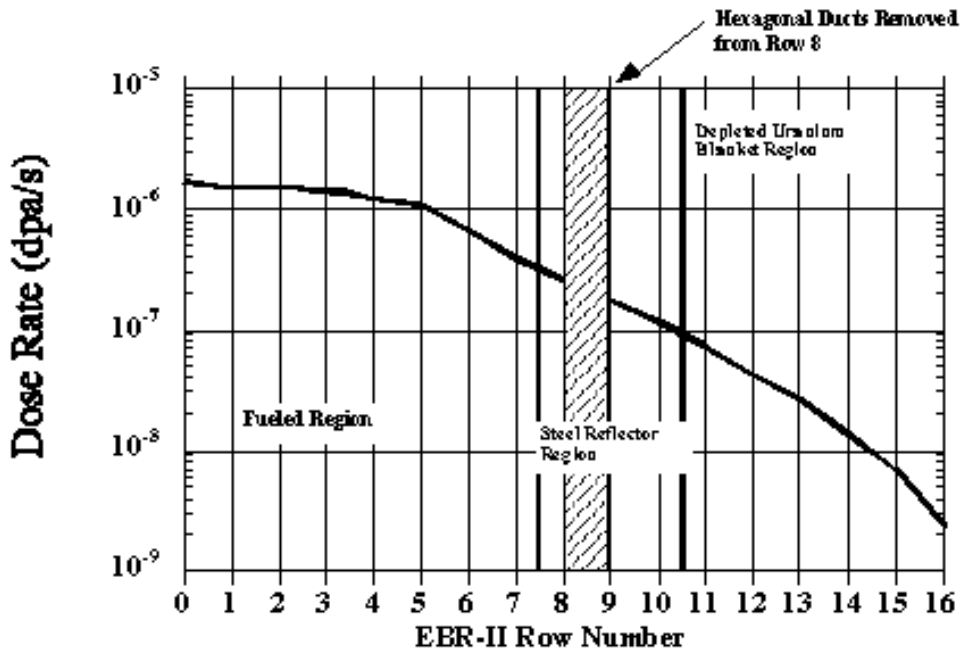


Figure 1. Dose rate as a function of axial position at core centerline in EBR-II.

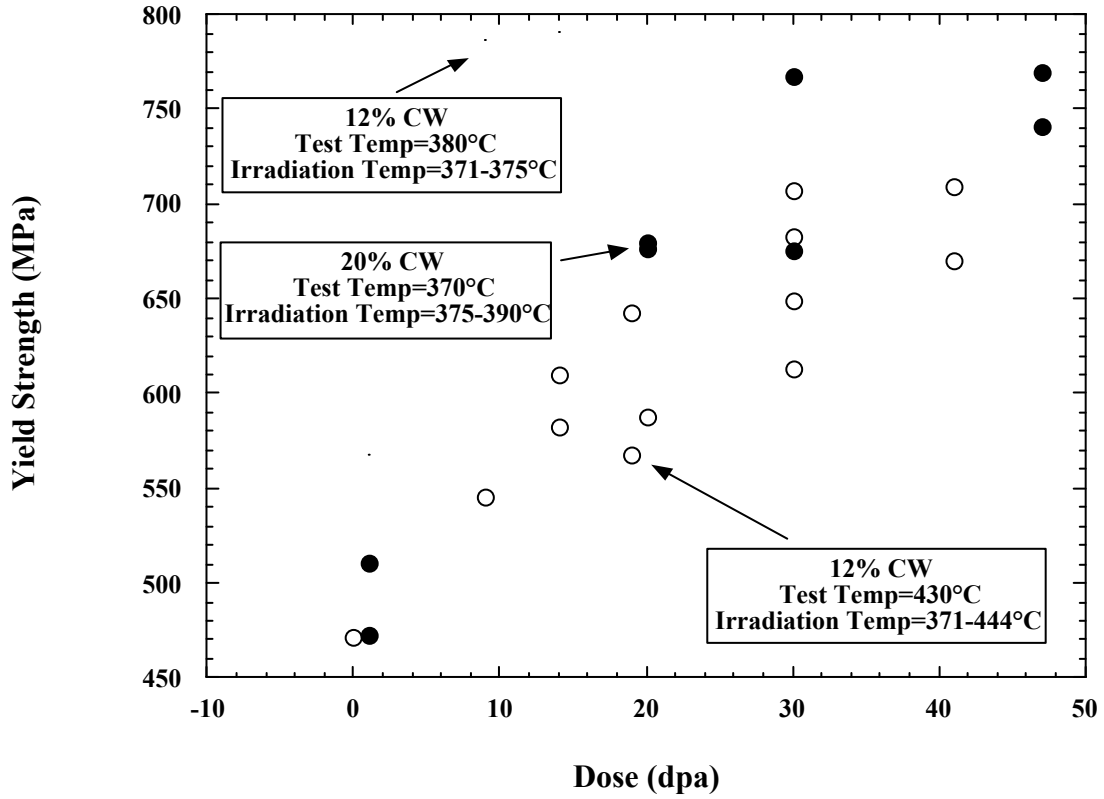


Figure 2. Yield Strength for EBR-II 316 stainless steel

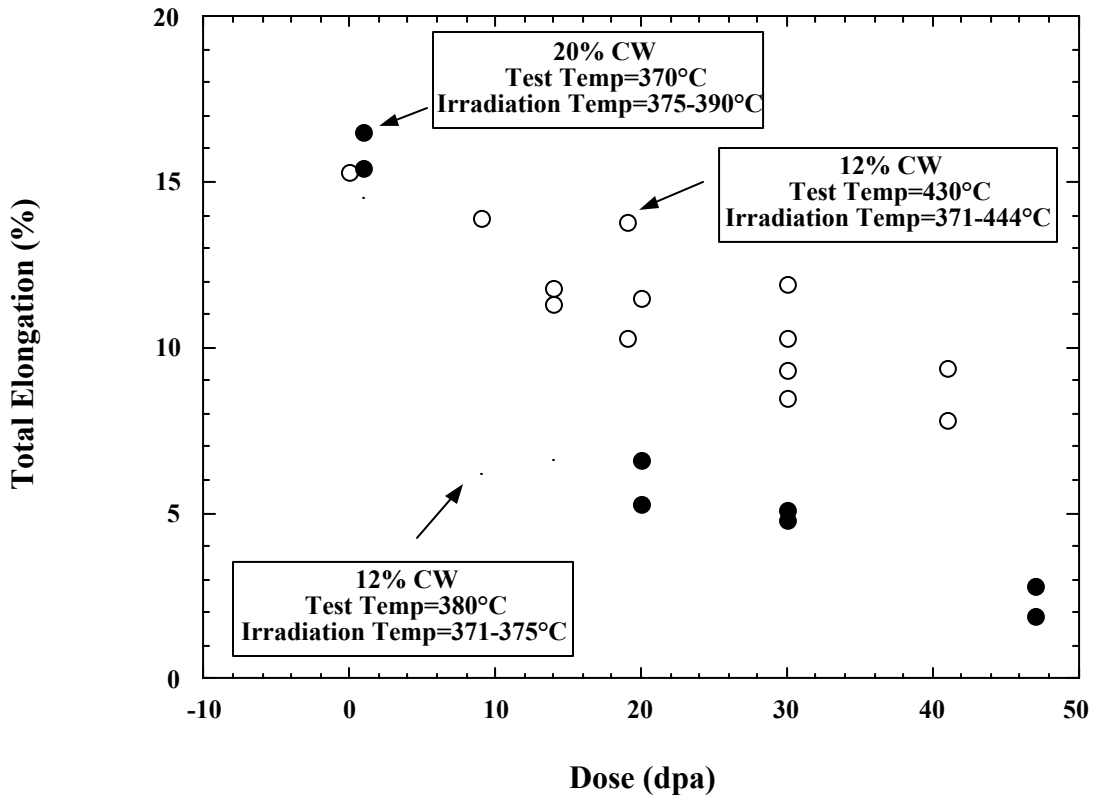


Figure 3. Total Elongation for EBR-II 316 stainless steel

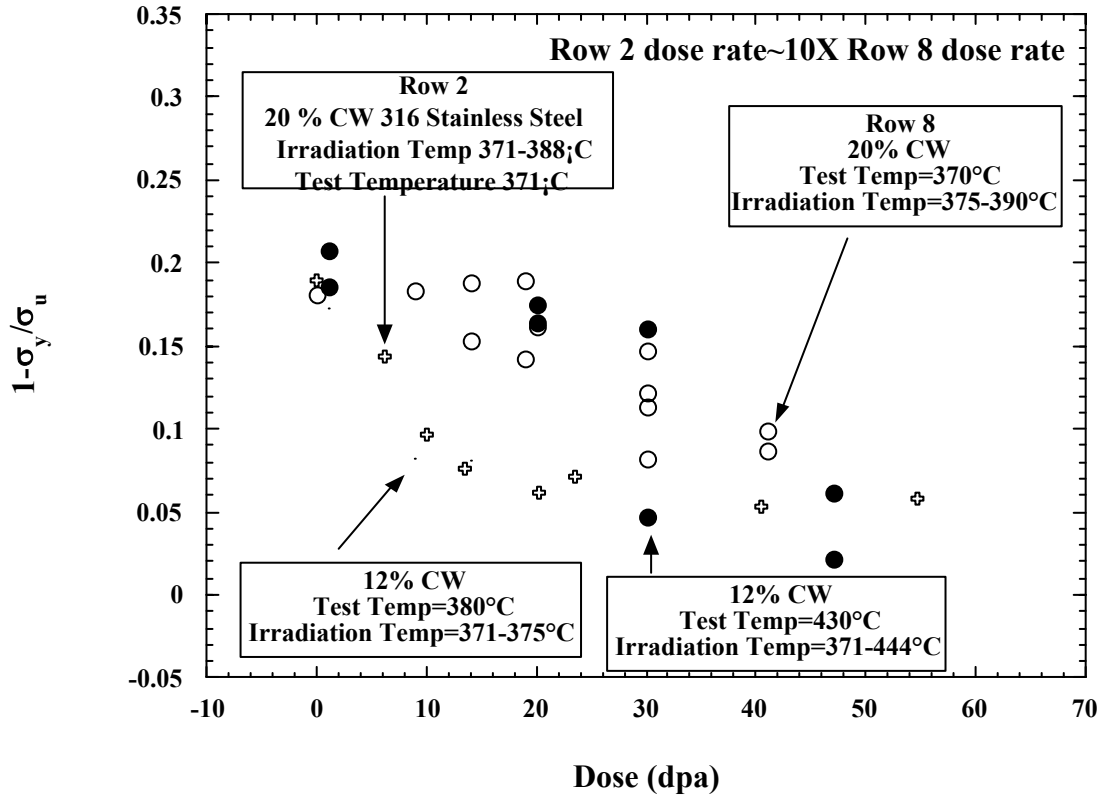


Figure 4. Hardening for EBR-II 316 stainless steel

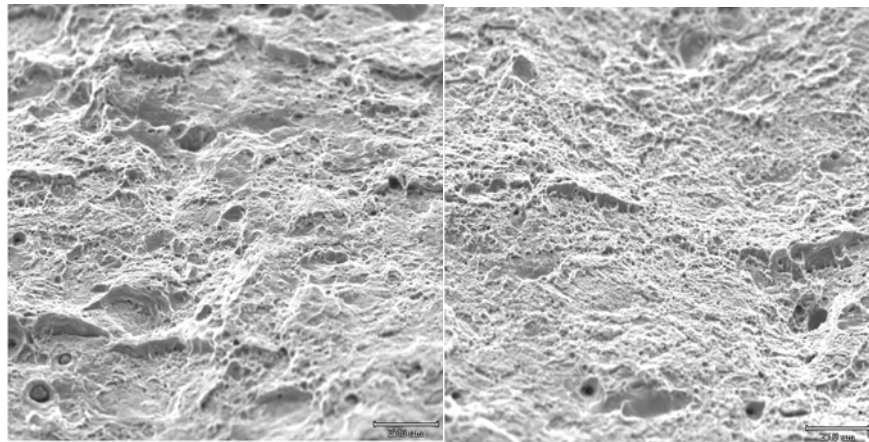


Figure 5 - Areas of fracture surface in 20% cold-worked 316 irradiated to 30 dpa showing ductile dimples mixed with facets.

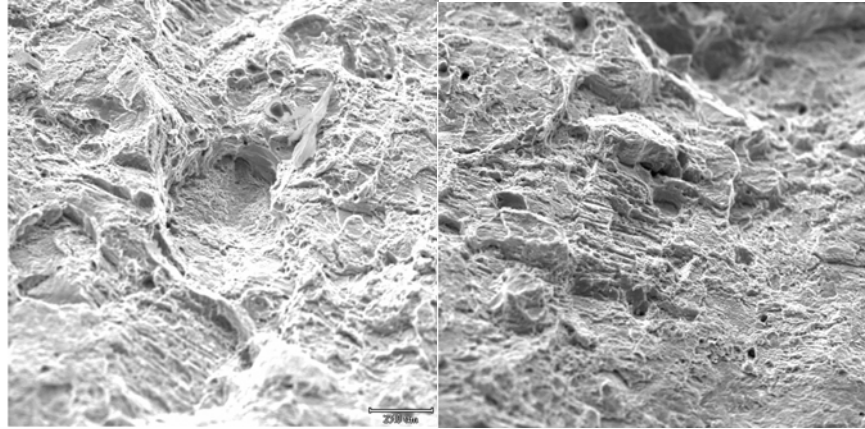


Figure 6 - Areas of fracture surface in 20% cold-worked 316 irradiated to 47 dpa showing a channel faceted surface.

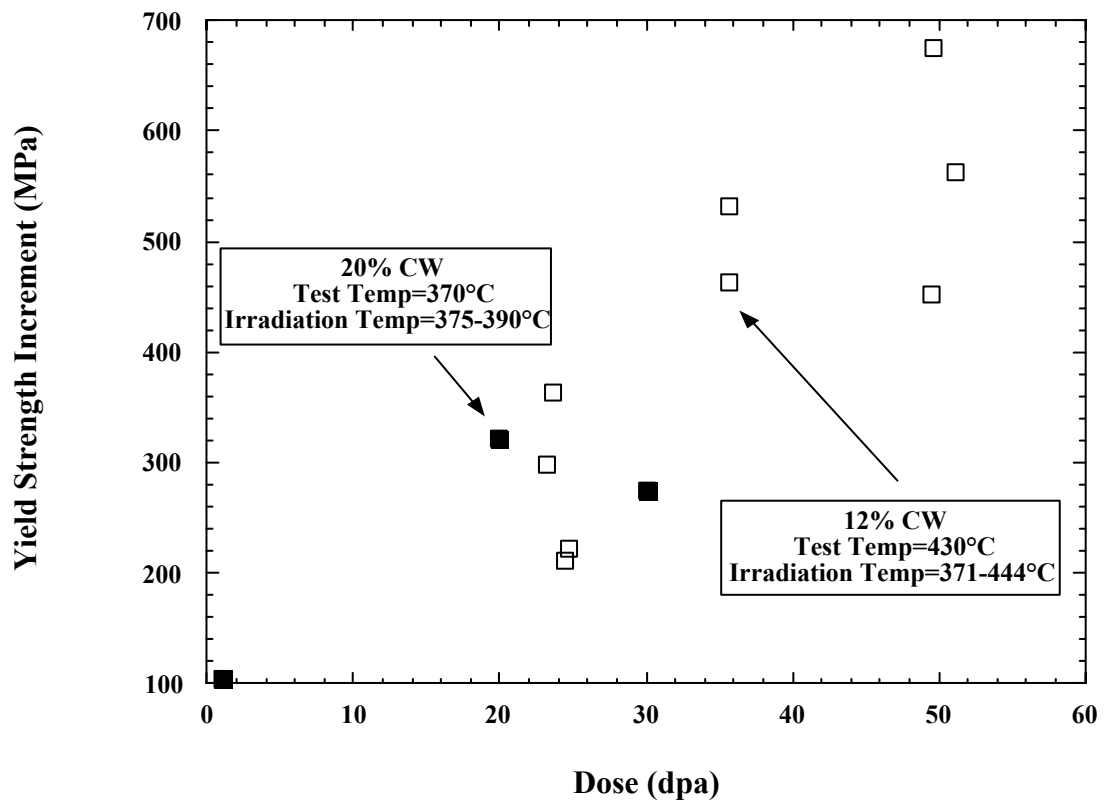


Figure 7. Hardening from voids and Frank loops for EBR-II 316 stainless steel